Application of a HV bipolar square-wave voltage generator for qualification and assessment of energy equipment

Rico Fischer-Baeumer[1], Kai Göhrmann[1], Konrad Domes[2], Benjamin Sahan[1], Christian Staubach[1]

[1]Hochschule Hannover
University of Applied Sciences and Arts
Ricklinger Stadtweg 120
30459 Hannover, Germany

[2]SAXOGY POWER ELECTRONICS
Dittesstr. 15
09126 Chemnitz, Germany

E-Mail: kai.göhrmann@hs-hannover.de, rico.fischer-baeumer@hs-hannover.de, benjamin.sahan@hs-hannover.de, christian.staubach@hs-hannover.de, info@saxogy.de

Keywords

Partial discharge, Modular Multilevel Converters (MMC), Cascaded H-Bridge, Insulation, Condition monitoring

Abstract

The increasing use of wideband gap devices poses a major challenge for the insulation system of motor windings due to its steep dv/dt voltage slopes. This paper focuses on the application of a modular bipolar square-wave voltage generator, which was built at the Hochschule Hannover and is now used in the high-voltage lab. Exemplary measurement results related to qualification and condition monitoring are presented. It is shown that the stress of a bipolar square-wave with high frequency and steep voltage slopes on the insulation system is much higher compared to a standard sinusoidal 50 Hz wave.

1 Introduction

Due to ongoing developments in power electronics [1] and new power conversion technologies [2, 3], the insulation system of energy equipment, such as rotating machines, cables, transformers, bushings, etc, is increasingly stressed by inverter voltage pulses. Especially the advancing of fast switching wide bandgap devices must be considered by the providers of isolation materials such as lacquer ectara. It is known, that the repetition frequency, peak-to-peak-voltages and voltage gradient during switching have a major influence on specific parts of the insulation system [4]. In comparison to LV-insulation systems, only limited knowledge is present regarding performance and aging of MV- and HV-insulation systems. However, the steep dv/dt voltage slopes may lead to an accelerated aging of the insulation system [5, 6]. Partial discharges may occur, which not only damage the machine or lead to spontaneous failure, but also may represent a health hazard for people [7]. Therefore, the need to investigate ageing behaviour of insulation materials in MV- and HV-Inverter applications is increasing. Consequently, a test device is needed that simulates the pulsed voltages in inverter operation realistically. This paper focuses on isolation materials of twisted pairs and insulation systems for rotating machines. In a first step a short introduction to a built bipolar square-wave voltage generator is given and the challenges with capacitive loads and their short circuit behaviour are investigated. Further the effects of a square-wave voltage on twisted pairs and insulation systems of generator bars are discussed. The differences between sinusoidal and square-wave stress on these insulations systems are shown.

2 Modular bipolar square-wave voltage generator

The topology used for the following tests is based on the well-known concept of cascaded H-Bridges as shown in Fig. 1 [8]. Each of these power stages uses a DC-Link voltage of V_d = 1200 V and a 1700 V IGBT H-Bridge module (see [9]) to generate a bipolar square-wave with a peak-to-peak voltage of $V_{pp} = 2400\,\mathrm{V}$. This is achieved by switching the individual IGBTs in the H-Bridge module complementary. Multiple of these power stages can be connected in series to increase the output voltage to the desired level. This way the DC- potential of one power stage matches the DC+ potential of the

stage below it. The output voltage of the inverter consequently results in the sum of all the DC-link voltages: $\pm V_\mathrm{d} \cdot n$, with n being the total number of power stages. The stages need to be isolated to each other and to earth. To do so the AC power supply which powers the DC-Link capacity of all the stages is isolated through transformers followed by rectifiers. Both in combination provide the desired DC voltage to the DC-Link Capacitors of each power stage. Handling the coupling capacities of the transformers can be challenging as they lead to high stray currents, but this topic is out of scope for this paper.

All power stages are controlled by a single microcontroller, which generates the necessary control signals to switch the IGBTs of each power stage complementary and at the same time. These control signals are transmitted via an optical fiber to each power stage to maintain the former mentioned electrical isolation. The square-wave generator used in this paper consist of four power stages. This results in a maximum output voltage of $V_\mathrm{out,max} = \pm 4800\ \mathrm{V}$ respectively $V_\mathrm{pp,max} = 9600\ \mathrm{V}$. The risetime is adjustable by varying the gate resistors of each driver stage.

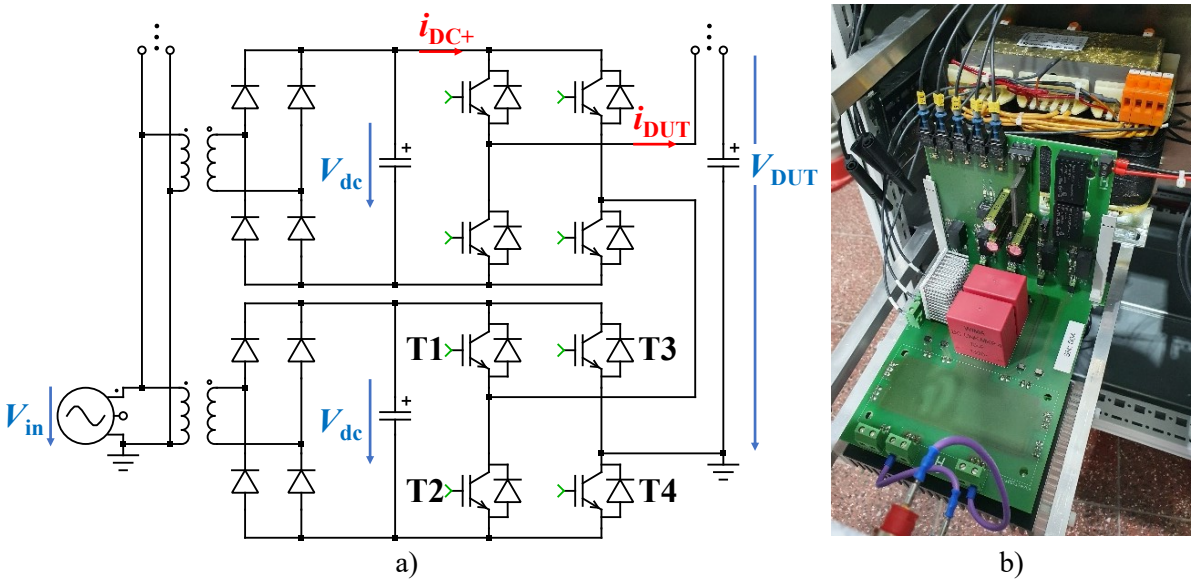

Fig. 1: a) Schematic of Modular square-wave generator and b) picture of one power stage

2.1 Switching characteristics under capacitive load

Typical datasheets of power semiconductors only list switching losses for currents as low as 10 % of the nominal current and inductive load. When testing insulations systems, the DUT typically behaves like a capacitive load with high ohmic resistance. Therefore, the currents experienced by the power semiconductor in this use case are not represented by the datasheet values. However precise values are needed to conduct simulations in development and for later thermal management of the power semiconductors.

To obtain better understanding of the switching losses under capacitive loads the IGBT module of one power stage is characterized with discrete capacitors with 55 pF, 100 pF, 1 nF and 3,3 nF as a load. The pF capacitors demonstrate the load of multiple twisted pair DUTs. The nF capacitors are in range of the capacitance of a generator bar. The rise time is set to approximately 150 ns and V_d to 1200 V. Furthermore, the IGBT module is tested at 100 °C to simulate operating conditions.

To analyze the dynamic losses the DC-link current ($i_\mathrm{DC+}$, see fig. 1a) is measured with a Rogowski coil [10]. Additionally, the DUTs current are measured with a Pearson probe and the voltage above the IGBT and the DUT by differential probes [11–13]. To determine the needed Energy of the H-Bridge the product of the DC-link current and DC-link voltage of 1200 V is integrated. The switching losses are then estimated by evaluating the energy balance. Therefor the energy stored on the Capacitor $\int |V_\mathrm{DUT}| \cdot i_\mathrm{DUT}$ is subtracted from the previously determined DC-link energy. The difference is the switching losses of the IGBTs. The results of this procedure are shown in figure 2. The DC-link currents of the different capacitances are shown in figure 2a) and the corresponding energies in 2b). It is visible

that the currents during the switching process are not negligible and therefore neither are the resulting losses. While aiming for a high frequent switching frequency these losses add up rapidly, even if they are in order of magnitude 10 times smaller than the minimum losses in the datasheet. This shows that an appropriate cooling system is needed at high switching frequencies and capacitive load.

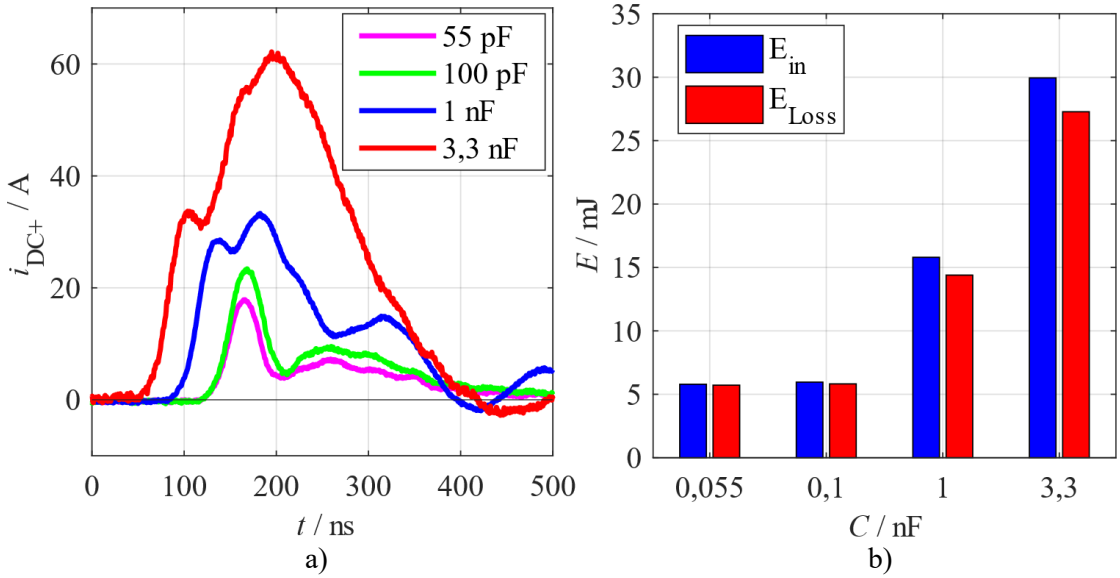

Fig. 2: a) DC-link current i_{DC+}, and b) corresponding input energy and loss energy per switching cycle of one H-Bridge

2.2 Breakdown behavior of the capacitive load

To analyze the lifetime of the test specimens, their breakdown behavior must be examined. In the worst case, they fail in a low ohmic short circuit. While the first laboratory prototype still employs standard IGBTs the usage of new SiC-MOSFET is planned. However, these devices show much lower short-circuit robustness. Typical allowable short circuit pulse duration is in the range of 2-3 µs.

As short circuit protection a shunt to measure the current in the DC- path in combination with a fixed voltage comparator is used as suggested in [10]. In contrast to typical gate drivers with DESAT-detection this approach allows a faster and more flexible protection.

An alternative over current protection is the use of melt-down fuses. This approach comes with ease of use but has several disadvantages: Each DUT needs its own separate fuse, and each fuse must be capable of withstanding the high frequency and high du/dt testing voltage in its entirety. This voltage can be several thousand Volt with rise times of 100 ns or less and as well as more than 20 kHz. Another disadvantage is that each fuse added to the testing setup also adds more parasitic inductance and capacity.

To investigate the breakdown behavior the following test procedure is used: Initial measurement with a double pulse to show the behavior under square-wave voltage stress when the DUT is known to be good. Afterwards the DUT is tested until end of life using accelerated aging with a high voltage AC source. Finally, the destroyed DUT is again tested with a double pulse square-wave voltage. For this test a single SiC-MOSFET H-Bridge is build using two 1200 V half-bridge modules [14]. This procedure is repeated for five test specimens.

Figure 3a) displays the initial measurement with a DC-link voltage of 900 V. All five DUTs show very similar characteristics here. The current wave form experiences a spike when the H-Bridge switches its polarity from -900 V to 900 V. The output current shows a short oscillation formed by the resonant tank of the capacitive twisted pair DUT and the cable inductance (length ~ 20 cm). This behavior represents the expectations.

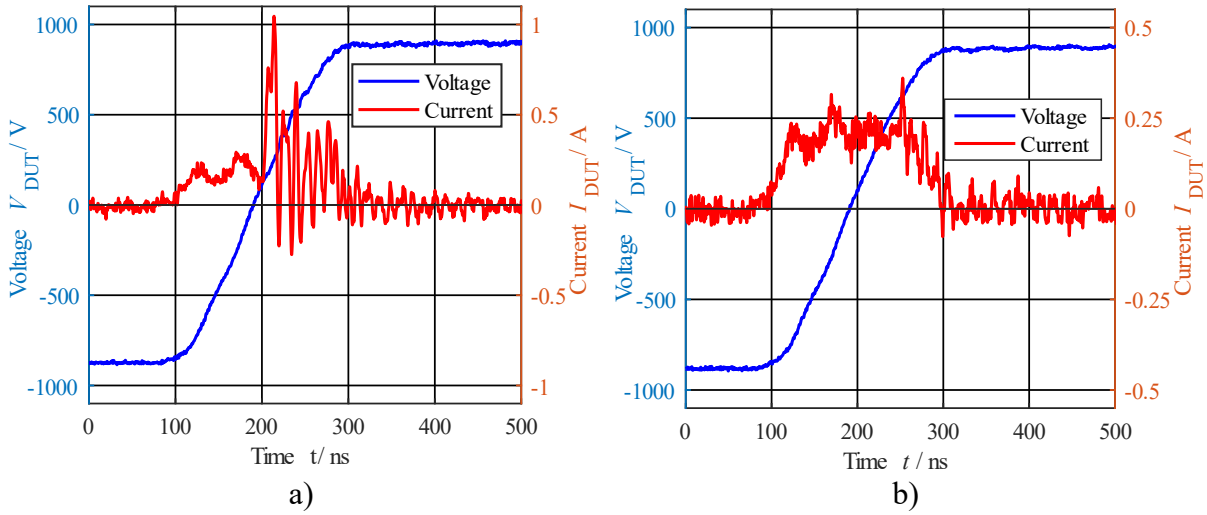

Fig 3: Voltage and current wave forms a one DUT a) before and b) after destruction but below breakdown voltage

After destroying the five DUTs a strong variation of the breakdown voltage has been observed. This can be explained by the length of the gap between the two strains of wire of the DUT where the defect accrued. Depending on the position of the defect the two strains of wire can be closer together or wider apart and the corresponding length of this gap and the air humidity while testing results in different breakdown voltage of the defect site of each DUT. Figure 3b) shows the waveforms of the DUT after the end-of-life test. No major abnormalities in the voltage and current wave forms compared to its intact state in Fig 3a) can be observed when setting the DC-link voltage to 900 V.

In contrast to this Fig. 2 shows the waveforms of a different DUT after destruction at a DC-link voltage V_d = 645 V. The insulation of the DUT breaks down and a low ohmic short circuit occurs. The current rises fast and reaches a peak value of 870 A before being shut down by the short circuit protection. The di/dt is only limited by parasitic inductance of the setup. It can be observed that the short circuit pulse duration is below 1µs which is well within the specification of the datasheet. However, no specific allowable number of short circuit events is specified in the datasheet and a case specific assessment between supplier and end user is necessary as stated in [15]. All tests are carried out at an ambient temperature of 22.5 °C and with a relative humidity of 31.3 %.

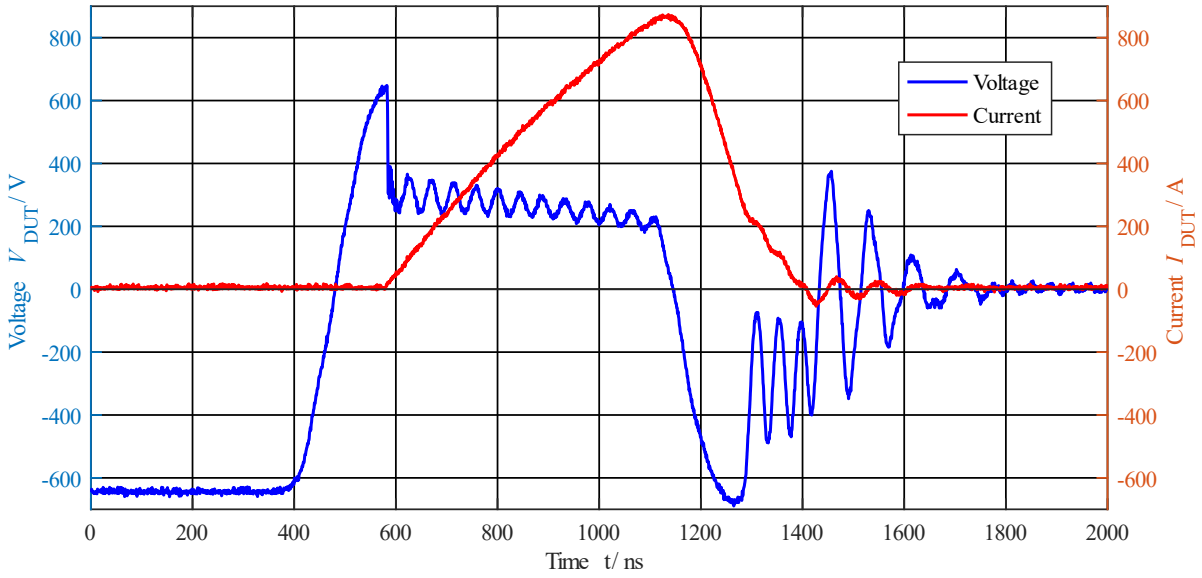

Fig 4: Current and voltage wave forms of short circuit operation of a twisted pair DUT

3 Influence of square-wave voltage with high dv/dt on the insulation of rotating machine windings

The characteristic inverter parameters used to drive rotating machines, i.e. repetition frequency, peak-to-peak-voltages and voltage gradient during switching can have a severe influence on specific parts of the insulation system [16, 17]. In comparison to LV-insulation systems, only limited knowledge regarding performance and aging of MV- and HV-insulation systems is available. Following some examples for application of the developed generator are presented.
A main challenge is to adjust the resulting stress for the individual DUT´s load. The resulting capacity and the parasitic inductivities can lead to oscillation voltages and currents and therefore imposes extra stress on the DUTs. It must be pointed out that the voltage of the unloaded square-wave generator is not comparable to the voltage with DUTs connected to it regarding voltage gradient and amplitude. In addition, the destruction of one or more DUT during the test may change the circuits behaviour as well and thereby changing the test conditions for the remaining DUTs.

3.1 PD-resistant HV-insulation system qualification – IEC 60034-18-42

In this case study a qualification of the stress grading system according IEC 60034-18-42 is presented [17]. It is known from other works, that especially the stress grading system of HV-insulation systems is exposed to high thermal and electrical stresses compared to AC operation [18–20]. This is mainly due to the conductive and semi-conductive materials used for electric field control in the slot and end-winding region [21]. Figure 5 shows the measurement setup for the stress grading system qualification according to IEC 60034-18-42. In this example 4 stages of the square-wave generator are used, which enables a maximum peak-to-peak voltage of about 9.6 kV.

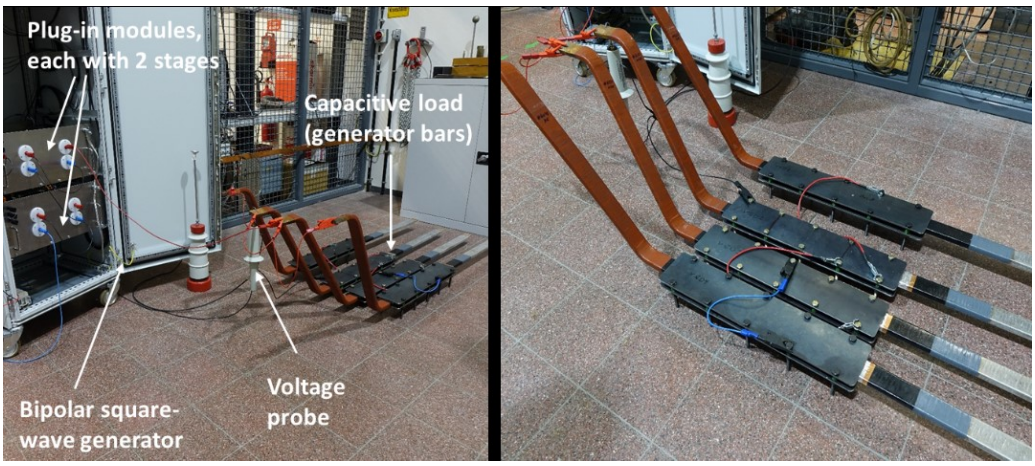

Fig. 5: Measurement setup for qualification according to IEC 60034-18-42

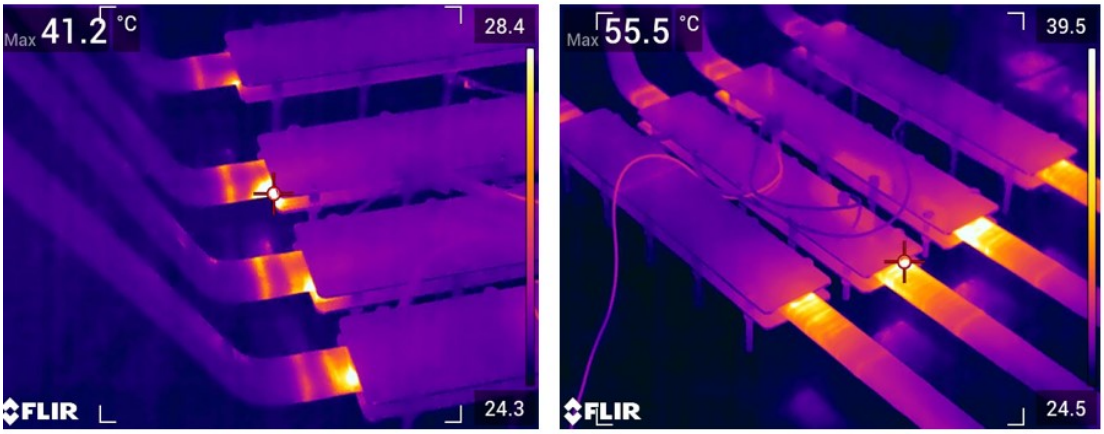

Fig. 6: Thermal images of both bars end indicating the areas exposed to the highest electric and thermal stresses caused by the inverter voltages at 1 kHz

Figure 6 presents thermal images of the test samples with clear hot-spots generated at the slot-exit area. This is mainly due to the high displacement currents generating ohmic loses in the conductive and semi-conductive materials even at quite low switching frequencies around 1-2 kHz.
As a result of these thermal stresses the insulation system is highly stressed and can age quite fast. By means of an UV-camera partial discharge activity is observable at the locations with the highest stress. This will result in visible deterioration due to chemical reactions and, see Figure 7.

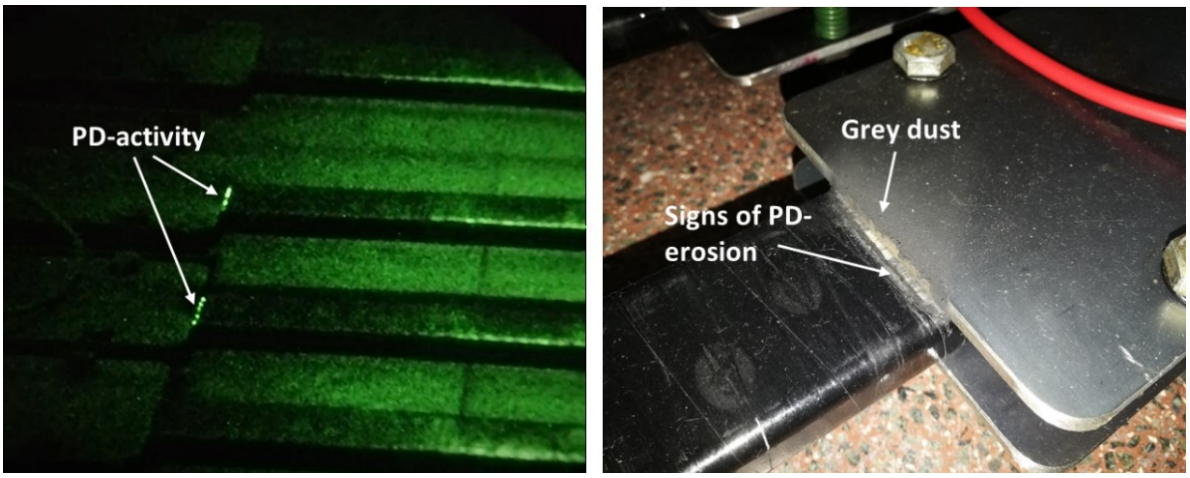

a) b)

Fig. 7: a) Partial discharge (PD) activity during qualification with the bipolar square-wave generator detected via an UV-camera and b) visible deterioration of the insulation system

Additionally, due the characteristic of the developed generator, the influence of the most important parameters, such as peak-to-peak-voltage and switching frequency, on the resulting electric and thermal stress can be investigated. The graph in Figure 8 gives the results of the temperature increase at the bar hot-spot area depending on the peak-to-peak-voltage for different repetition frequencies. At higher voltages it is only possible to apply smaller frequencies due to the risk of burning caused by excessive loses in the HV-insulation system. The graph in figure 8 points out, that there is a quite significant influence of repetition frequency on the resulting temperature increase i.e., thermal stress.

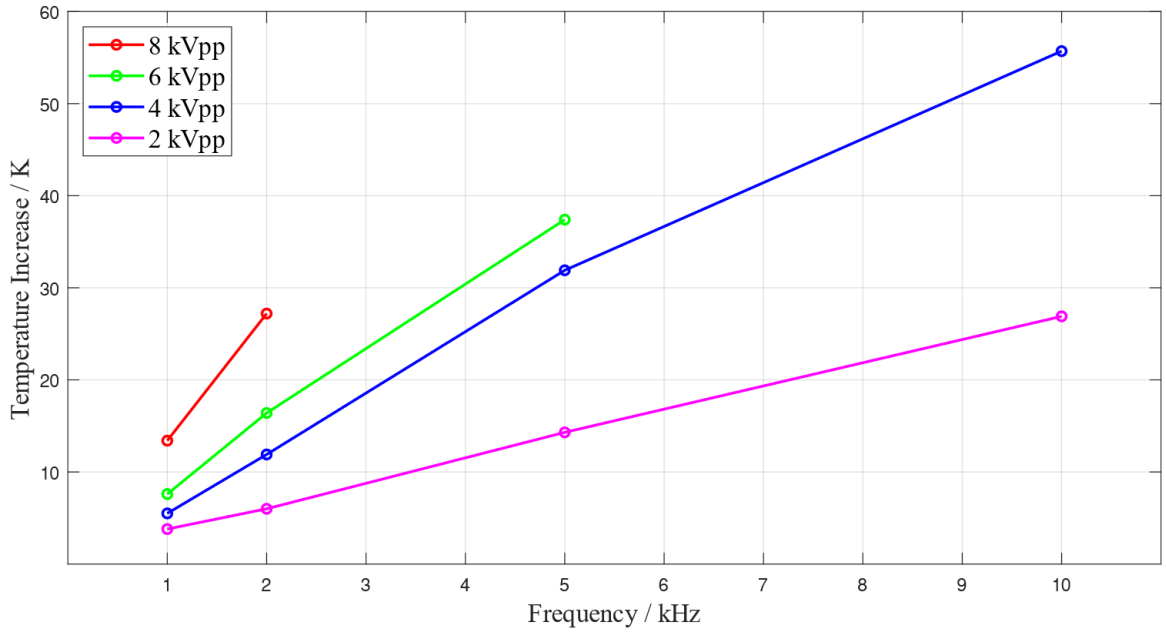

Fig. 8: Influence of repetition frequency on the temperature increase in the stress grading area

3.2 LV-wire insulation lifetime testing and PDIV of twisted pairs under square-wave and sinusoidal voltage

Another application of the developed bipolar square-wave generator is the wire insulation lifetime testing according to IEC 62068 [22]. twisted pairs are stressed with repetitive voltage impulses. The objective is to quantify the electric lifetime of the wire insulation for a given electric stress, the repetition frequency goes up to 20 kHz. Recommendations for appropriate voltage parameters are currently in discussion [23]. The twisted pair with the connections and the applied voltage is shown in Figure 9. Due to the field concentration between the wires quite significant PD-activity is generated at the triple-junction locations. Figure 10 presents visible and figure 11b) UV-pictures of the twisted pair during testing.

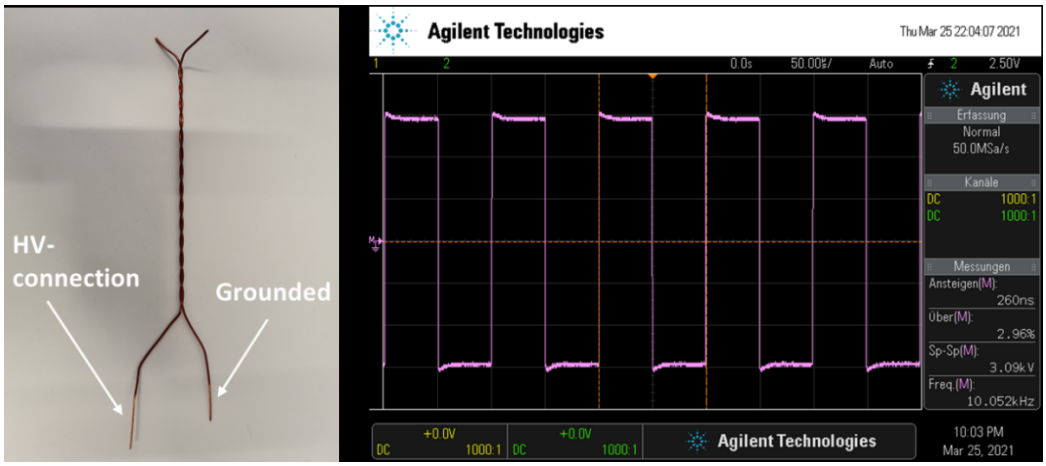

a) b)

Fig. 9: a) Twisted pair and b) applied repetitive voltage impulses

To investigate the influence of square-wave voltage on PDIV five DUTs were placed on a retainer and stressed with square-wave voltage with 100 ns risetime and 20 kHz switching frequency. The PDIV for each of the five DUTs is noted separately. To have a comparison the same test is carried out again but this time using 50 Hz sinusoidal voltage.

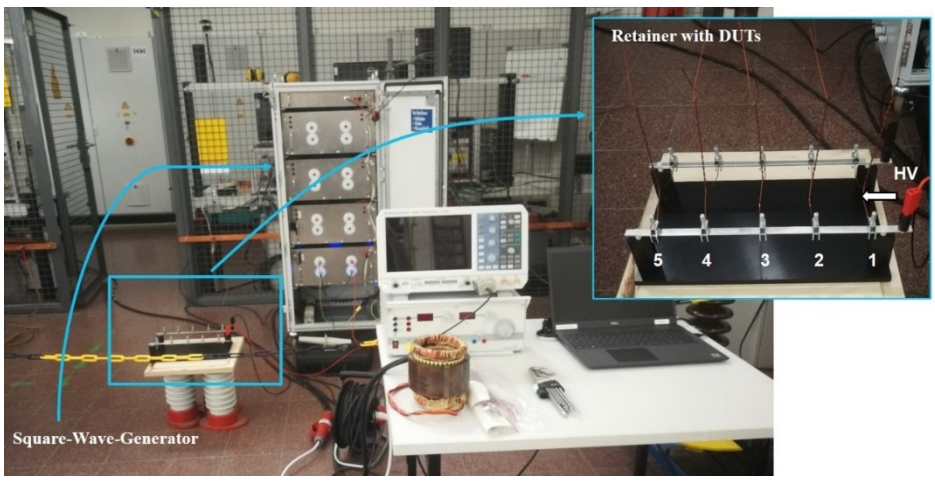

Fig. 10: Testing setup used for application of square-wave voltage

Under square-wave voltage stress the DUTs show vastly different PDIV. The peak-to-peak value of the PDIV is ranging from 1.46 kV to 1.67 kV. In comparison the PDIV while sinusoidal voltage is applied is uniform at the same voltage of 1.78 kV. It is noteworthy to point out that the PDIV is from 0.11 kV to 0,32 kV lower when the DUTs are stressed with square-wave voltage. Figure 11a) shows the PDIV for each of the five DUTs. Another noteworthy discovery is that in addition to the fact that each DUT has a different PDIV the corona discharge of each twist of one individual DUT is also not uniform when

a square-wave voltage is applied. This can be seen in figure 11b). A voltage of 1.6 kV is applied to the retainer and therefore to each DUT. In accordance to figure 11a) DUT number 1 – 3 show no corona discharge as they are below the PDIV. DUT 4 and 6 show nonuniform corona discharge and even spots in the middle where no corona can be observed.
This concludes in the realization that the inherent structure of a twisted pair may not be ideal for lifetime testing of insulation systems and another testing method hast to be developed and adopted to achieve conclusive results.

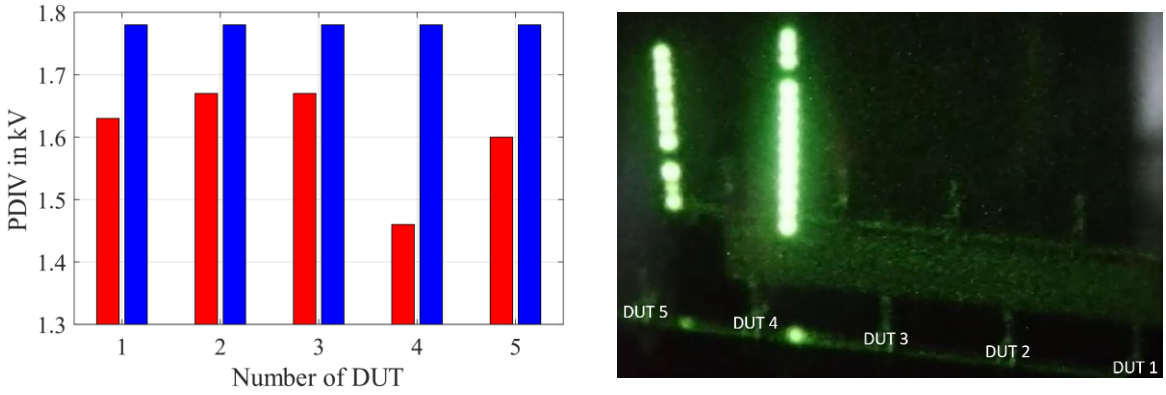

a) b)

Fig. 11: a) PDIV of all five twisted pair DUTs under square-wave (red) and sinusoidal stress (blue), b) Nonuniform corona discharge of individual twists of a twisted pair DUT (same Voltage applied)

3.3 Offline PD-measurement with repetitive, impulse voltage

Comparable to the IEC standard for offline partial discharge measurements of rotating machines with sinusoidal voltages for condition assessment [24] currently a new standard related to repetitive impulse voltage excitation is discussed [25]. First investigations in our lab were conducted, see Figure 12. However, the challenge is not to generate but to measure the partial discharge activity accurately. This is due to the fact, that the expected frequency content of the partial discharge events is in similar range to the repetitive impulse voltage. Also, oscillation is likely to occur distorting the measurement results may occur. Therefore, further work is needed regarding this topic. Especially, precise boundary conditions and general guidelines in the relevant standard might be necessary.

a) b)

Fig. 12: a) Measurement setup acc. to IEC 60034-27-5 and b) measurement results (yellow: square-wave voltage, green: measured voltage of the measurement quadrupole, orange: output of PD activity channel of the measurement quadrupole

4 Conclusion

The approach of testing different insulation materials using a modular, cascaded H-Bridge voltage generator shows clear results. The stress caused by using square wave voltage differs from the stress caused by sinusoidal voltage. Especially generator bars experience a high-level thermal stress, which gets visible through the thermal imaging camera as well as the resulting grey dust. This increased stress is caused by high voltage slopes and the high switching frequency of the square-wave voltage. Standard partial discharge measurement is not possible without problems. This results in the need for further work regarding this topic.
Additionally, requirements for building a square-wave voltage generator are shown. At first, a superior short circuit detection is needed. Otherwise save operating conditions cannot be guaranteed and the low ohmic short circuit can easily destroy the power semiconductors. In addition, an adequate cooling solution for the power semiconductors is highly recemented as the switching losses under capacitive load cannot be ignored. Especially while testing generator bars with high capacity and high frequency. All these findings show clear trends and challenges, which will require further investigations.

5 Acknowledgements

This research project was carried out in the framework of the industrial collective research program ZIM. It was supported by the Federal Ministry for Economic Affairs and Climate Action (BMWK) through the AiF (German Federation of Industrial Research Associations eV) based on a decision taken by the German Bundestag. The authors would like to thank Stefan Reddig for his support.

6 References

[1] K. Bae et. al., *Current State and Development Trends of Insulation Systems in BEV Traction Motors Steered by Electric Powertrain Innovation: International Exhibition and Conference for Power Electronics, Intelligent Motion, Renewable Energy and Energy Management Proceedings, 3 - 7 May 2021*. Berlin: VDE Verlag, 2021.
[2] T. Hildinger, “Frades II- Europe’s Largest and Most Powerful Doubly Fed Induction Machine, HydroVision International,” Charlotte, NC, USA, 2018.
[3] C. Staubach and T. Hildinger, “Innovative Technologie eines drehzahlvariablen Pumpspeicherkraftwerks unter Berücksichtigung des hochspannungstechnischen Isoliersystems, Generatoren in konventionellen Kraftwerken, Windparks und Wasserkraftwerken,” 14. Essener Tagung, 2020.
[4] *Rotating electrical machines – Part 18-42: Partial discharge resistant electrical insulation systems (Type II) used in rotating electrical machines fed from voltage converters - Qualification tests*, IEC 60034-18-22, 2017.
[5] Institute of Electrical and Electronics Engineers, *2020 IEEE Electrical Insulation Conference (EIC)*. Piscataway, NJ: IEEE, 2020.
[6] Marco Denk and Mark-M. Bakran, “Partial Discharge Measurement in a Motor Winding fed by a SiC Inverter – How critical is high dV/dt really?: PCIM Europe 2018; International Exhibition and Conference for Power Electronics, Intelligent Motion, Renewable Energy and Energy Management,” pp. 1–6, Jun. 2018,
[7] R. Bartnikas, “Partial discharges: Their mechanism, detection and measurement,” vol. 9, no. 5, pp. 763–808, 2002.
[8] Peter W. Hammond, “MEDUMVOLTAGE PWM DRIVE AND METHOD,” 5,625,545, Apr 29, 1997.
[9] Infineon, Ed., “F4-100R17N3E4 Datasheet: EconoPACK™3modulewithTrench/FieldstopIGBT4andEmitterControlleddiodeandNTC,” May. 2015.
[10] PEM Datasheet, “CWT Mini,” 2020.
[11] Sapphire Instruments Datasheet, “SI-9010A Specifications,”
[12] PMK Datasheet, “BumbleBee®,” 2020.
[13] Pearson Electronics, INC. Datasheet, “Pierson_Sonde_2877,”

[14] Infineon, Ed., “FF11MR12W1M1_B11 Datasheet: EasyDUALmodulewithCoolSiC™TrenchMOSFETandPressFIT/NTC,” Jul. 2018.
[15] Z. Yuan, I. Voss, P. Salmen, T. Aichinger, R. Elpelt, and P. Friedrichs, “How Infineon controls and assures the reliability of SiC based power semiconductors (Whitepaper): Whitepaper,”
[16] *Rotating electrical machines: Part 18-42: Partial discharge resistant electrical insulation systems (Type II) used in rotating electrical machines fed from voltage converters - Qualification tests*, IEC 60034-18-41, 2017.
[17] *Rotating electrical machines: Part 18-42: Partial discharge resistant electrical insulation systems (Type II) used in rotating electrical machines fed from voltage converters - Qualification tests*, IEC 60034-18-42, 2017.
[18] C. Staubach and T. Hildinger, *Stress grading system evaluation for a converter feed hydro generator winding: IEEE Electrical Insulation Conference (EIC)*. Knoxville, TN, USA: IEEE, 2020.
[19] E. Sharifi-Ghazvini, *Analysis of Electrical and Thermal Stresses in the Stress Relief System of Inverter Fed Medium Voltage Induction Motors*. PhD Thesis, University of Waterloo. Ontario, Canada, 2010.
[20] J. Wheeler, “Effects of converter pulses on the electrical insulation in low and medium voltage motors,” *IEEE Electrical Insulation Magazine*, vol. 21, no. 2, pp. 22–29, 2005, doi: 10.1109/MEI.2005.1412216.
[21] B. Marusic, “Efficiency Evaluation of Semiconducting Stress Control System: IEEE Electrical Insulation Conference (EIC),” Pittsburgh, PA, USA, 1994.
[22] *Electrical insulating materials and systems - General method of evaluation of electrical endurance under repetitive voltage impulses*, IEC 62068:2013.
[23] *Winding wires - Test methods - Part 7: Electrical endurance under high frequency voltage impulses*, IEC 60851-7.
[24] *Rotating electrical machines – Part 27-1: Off-line partial discharge measurements on the winding insulation*, IEC 60034-27-1, 2017.
[25] *Rotating electrical machines – Part 27-5: Off-line partial discharge measurements on winding insulation of rotating electrical machines during repetitive impulse voltage excitation*, IEC 60034-27-5, Draft.